Amphiphilic Gradient Copolymers Shape Composition Influence on the Surface/Bulk Properties

Khaled Karaky,[†] Laurent Billon,*[,†] Claude Pouchan,[‡] and Jacques Desbrières[†]

Laboratoire de Physico-Chimie des Polymères, UMR 5067 CNRS, Université de Pau et des Pays de l'Adour, Laboratoire de Chimie Théorique et Physico-Chimie Moléculaire, UMR 5624 CNRS, Université de Pau et des Pays de l'Adour, Hélioparc 2, Avenue du Président Angot, 64053 Pau Cedex, France

Received October 24, 2006; Revised Manuscript Received December 5, 2006

ABSTRACT: Nitroxide-mediated radical polymerization (NMP) combined with the semibatch process was used to synthesize poly(*N, N*-dimethylacrylamide-*grad*-butylacrylate), called poly(DMA-*grad*-BuA), in the presence of SG1 as a control agent and the alkoxyamine (MAMA) as an initiator. The pseudo-instantaneous composition was used to characterize the gradient copolymers. The variation of the addition rate of DMA influences the incorporation of DMA in the macromolecular chains. The preliminary surface characterization by the measure of the static water contact angle of the gradient copolymers films indicated that the monomer unit sequence in the polymer chain strongly influences the surface properties. The rheological properties of gradient copolymers in bulk were also studied and discussed in relation to their local structure.

Introduction

Poly(acrylamide) and its derivatives are an extremely important class of synthetic polymers widely used in industry.[1] They are found in numerous applications because of their biocompatibility and hydrophilic/water-soluble properties.[1,2] They were synthesized using ionic and free radical polymerization (FRP). Conventional FRP of acrylamide yields poorly defined polymers,[3,4] but recently, a range of well-defined polyacrylamides have been prepared by different controlled/living radical polymerization (CRP) methods as nitroxide-mediated radical polymerization (NMP),[5] atom transfer radical polymerization (ATRP),[5−8] and reversible addition−fragmentation chain transfer (RAFT).[9−12]

According to the literature, ATRP was widely used for preparing well-defined polyacrylamide. Indeed, Matyjaszewski et al. showed that DMA can be polymerized under controlled conditions, providing Me_6TREN as the ligand in conjunction with CuCl and an appropriate chlorinated initiator.[13] Later, Matyjaszewski et al. reported the homopolymerization of DMA by ATRP with molecular weight, $M_n = 50\,000$ g·mol^{-1}, while retaining a low polydispersity index ($I_p = 1.12$). These homopolymers of DMA were used to prepare both random and block copolymers of DMA and BuA.[14] Sawamoto et al. achieved previously controlled polymerization of DMA by ATRP, resulting in polydispersity higher than 1.6.[15]

Moreover, the RAFT was also used to prepare well-defined homopolymers and copolymers with DMA. In fact, Donovan et al. carried out the syntheses of the novel acrylamido-based RAFT chain transfer agents (CTAs) *N,N*-dimethylacrylamide-*S*-thiobenzoylthiopropionamide (TBP) and *N,N*-dimethyl-*S*-thiobenzoylthioacetamide (TBA) for the controlled polymerization of DMA.[11] Rizzardo et al. showed that PDMA-*b*-PS diblock copolymers could be obtained with a narrow polydispersity by chain extension, using ω-thiocarbonylthio-PS as an initiator and AIBN as a radical source.[16]

In addition, NMP is one of the oldest methods and remains increasingly interesting because the range of polymerizable monomers still broadens. In NMP, a growing polymer chain is reversibly terminated by a nitroxide (e.g., TEMPO, SG1), as shown in Figure 1. The CRP of DMA and acrylamido monomers in general has proven to be challenging using NMP. Indeed, Li and Brittain reported the polymerization of DMA by NMP using the TEMPO as a counter radical and AIBN as an initiator, but the process was not controlled.[17] Diaz et al. have synthesized PDMA and poly(4-vinylpyridine-*b*-*N,N*-dimethylacrylamide) in a controlled manner using a β-phosphonylated nitroxide, commonly designated as SG1 as a counter agent and the *N*-*tert*-butyl-*N*,1-diethylphosphono-2, 2-dimethylpropyl-*o*-1-phenylethylhydroxyamine (Sty-SG1) as an initiator.[18] Recently, Schierholz et al. have shown the synthesis of well-defined poly(DMA) and poly(DMA-*b*-BuA) in the presence of SG1 and AIBN as the initiator. The authors have shown that the free radical polymerization of DMA exhibits a living/controlled character using an excess of nitroxide radical (SG1).[19]

Unlike block and random copolymers, gradient copolymers represent a novel architecture of materials. The composition of gradient copolymers gradually changes from one end of the polymer chain to the other. Therefore, gradient copolymers have distinct properties.[7] Batch and semibatch copolymerization methods were used to form controlled gradient copolymers in instantaneous composition.[20−28] Recently, we have focused our activity on such a polymer structure to understand the effect of the synthetic methodology on the molecular architecture and the intrinsic properties of the monomer on their surface structures.[25,28]

The objective of this work consists of the syntheses of gradient copolymers poly(DMA-*grad*-BuA) by coupling a hydrophilic monomer (DMA) with another hydrophobic one (BuA) having a low glass transition temperature (T_g). We report here for the first time the synthesis of gradient copolymers poly(DMA-*grad*-BuA) by semibatch nitroxide-mediated controlled radical polymerization using a alkoxyamine (MAMA) as an initiator and an excess of SG1 as a control agent. We will show the ability of SG1 combined with the MAMA in a process in

* Corresponding author. E-mail: laurent.billon@univ-pau.fr.
[†] Laboratoire de Physico-Chimie des Polymères.
[‡] Laboratoire de Chimie Théorique et Physico-Chimie Moléculaire.

10.1021/ma062456s CCC: $37.00
Published on Web 01/10/2007

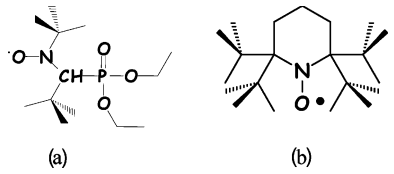

(a) (b)

Figure 1. Structure of the nitroxide deactivator in NMP: (a) SG1 and (b) TEMPO.

semibatch nitroxide-mediated polymerization to control the copolymerization of DMA with BuA. These copolymers synthesized by the semibatch process were obtained by continuous addition of DMA during the polymerization reaction of BuA. These copolymers will be characterized by various techniques, and we focused on their organizations at the surface and their structure/rheological properties relationship.

Experimental Section

Materials. *N*,*N*-Dimethylacrylamide (DMA, 99%) and butyl acrylate (BuA, 99%) were used as received from Aldrich. The alkoxyamine, 2-methylaminoxypropionic-SG1 (MAMA, 99%), as the initiator, and *N*-*tert*-butyl-(1-diethyl-phosphono-2,2-dimethyl-propyl) nitroxide (SG1, 88%), as the counter radical, were provided by Arkema Chemicals. All solvents and reagents were used as received without further purification.

Nuclear Magnetic Resonance Spectroscopy (NMR). Conversion of styrene and butyl acrylate and copolymer composition were determined by ^{1}H NMR in $CDCl_3$ on a Bruker 400 MHz instrument at room temperature.

Size Exclusion Chromatography (SEC). Molar mass and molar mass distribution of PDMA samples were determined at 30 °C using size exclusion chromatography. Characterizations were performed using a GPCV 2000 Waters Alliance system with aqueous solution ($NaNO_3$, 0.1 M and NaN_3, 5 ppm) as eluent at a rate of 0.5 mL/min. The chromatographic device was equipped with three Ultrahydrogel columns 250, 500, and 2000 working in series at 30 °C. The system was equipped with a capillary refractomer and differential viscosimeter detectors. A calibration curve was established with low polydispersity index linear poly(ethylene glycol) standards, and ethylene oxide was used as an internal standard for the system.

Copolymer molecular weights were determined at 40 °C using size exclusion chromatography (SEC). Characterizations were performed using a 2690 Waters Alliance system with THF as eluent at a rate of 1 mL/min. The chromatographic device was equipped with four Styragel columns HR 0.5, 2, 4, and 6 working in series at 40 °C, a 2410 refractive index detector and a 996 Waters photodiode array detector. A calibration curve was established with low polymolecularity index polystyrene standards, and toluene was used as an internal standard for the system.

Differential Scanning Calorimeter (DSC). Glass transition temperatures (T_g) were measured using a differential scanning calorimeter, (TA series-Q100). Samples (~10 mg) were weighed and scanned at 20°/min from −65 to 130 °C under dry nitrogen (50 mL/min). The reported values of T_g were determined from the second heating run and were taken as the middle point of the $\Delta H/\Delta T$ step in the DSC spectra.

Static Contact Angle Measurement. The sessile drop technique (TRACKER) was used to measure the static contact angle. Drops of pure water were prepared with a syringe and were dropped onto the surface of polymer films. The films were prepared on a glass slide with 1 mm thickness obtained under vacuum after a thermal treatment of 3 h at 90 °C and a slow temperature decrease over 5 h to room temperature. The measurements were carried out in a wet and closed controlled cell to avoid the evaporation of the water drop. The static contact angle was measured at contact time $t = 60$ s and was repeated at least three times, and the average value was shown as a data point.

Rheological Experiments. To observe some transitions, particularly the glass transition in this study, we have performed thermomechanical experiments (2°·min^{-1}), following the variation of G' (storage modulus) and G'' (loss modulus) at a fixed pulsation (1 rad·s^{-1}) in the temperature range from −50 to about 150 °C and using a Rheometrics RDA II rotational rheometer (Rheometrics, New Castle, DE). We have adapted the geometry, parallel−plate or rectangular torsion, according the level of the modulus of the sample at different temperatures and in order to minimize instrument compliance and/or slip effects.

Homopolymerization of DMA. In a 50 mL round flask, MAMA (0.077 g, $2.021\cdot10^{-4}$ mol), SG1 (0.004 g, $1.26\cdot10^{-5}$ mol), DMA (10 g, 0.101 mol) ([SG1]/[MAMA] = 6%), were dissolved in 23 mL of toluene, as described by Sawamoto.[15] The mixture was degassed by bubbling with nitrogen gas for 30 min. The flask was placed into an oil bath at 112 °C. Aliquots were sampled to determine conversion by ^{1}H NMR and molecular weight by SEC calibrated with PEG standards. After 3 h 10 min, the flask was cooled down to room temperature and exposed to air: 43% conversion (^{1}H NMR); M_n = 13 300 g/mol and I_p = 1.4. The polymer was precipitated in hexane, and the resulting solid was isolated by vacuum filtration and dried for 48 h under vacuum.

Semibatch Copolymerization of DMA with BuA by NMP. *a. Synthesis of Gradient Copolymer A (G_A).* The synthesis of this copolymer was prepared by semibatch nitroxide-mediated copolymerization. Indeed, into a first round flask, BuA (12.8 g, 0.1 mol) and 2-methylaminoxypropionic-SG1 (MAMA) (0.151 g, $3.96\cdot10^{-4}$ mol) as an initiator, an excess of SG1, [SG1]/[MAMA] ≈ 6%, and 19 mL of toluene were introduced, [BuA] ≈ 5.2 mol/L. The initiator was solubilized by stirring. The solution was degassed by nitrogen bubbling for 30 min. In another round flask, we introduced *N*,*N*-dimethylacrylamide monomer (9.7 g, 0.098 mol). The *N*,*N*-dimethylacrylamide monomer was degassed by nitrogen bubbling for 30 min, then DMA was transferred into an syringe. The first round flask (BuA solution) was placed in an oil bath at 112 °C; then as soon as the reaction temperature was reached, DMA was added (considered as $t = 0$ min). The semibatch polymerization was performed by addition of DMA using a pump with a rate of 1.4 mL/h. After 7 h 10 min, the DMA addition was complete, whereas the reaction was stopped after 7 h 20 min (10 min after end of DMA addition). From these experimental values, the classical ratio has been calculated [DMA-BuA]/[MAMA] ≈ 500.

Samples of the copolymerization mixture were withdrawn at periodic intervals, and conversion was determined by ^{1}H NMR spectroscopy, while molecular weights were determined by SEC calibrated with PS standards. The final polymer obtained was soluble in the THF, precipitated in hexane, and the resulting solid was isolated by vacuum filtration and dried for 48 h under vacuum. Monomer conversion was found to be 76% DMA and 88% BuA (from ^{1}H NMR). Average molecular weight and molecular weight distribution were measured using SEC at the final stage (M_n = 33 000 g/mol; I_p = 1.28).

b. Synthesis of Gradient Copolymer B (G_B). The experimental conditions were the same for this copolymerization except for the addition rate of DMA, which is 2.8 mL/h. After 3 h 35 min, the DMA addition was complete, whereas the reaction was stopped after 4 h. Monomer conversion was found to be 48% DMA and 62% BuA (^{1}H NMR). Average molecular weight and molecular weight distribution were measured using SEC calibrated with PS standards at the final stage (M_n = 24 000 g/mol; I_p = 1.24).

c. Gradient Copolymer C (G_C). As described above for the two first gradient copolymers, the experimental conditions were the same for this copolymerization except for the addition rate of DMA, which is 0.8 mL/h. After 13 h, the DMA addition was complete, whereas the reaction was stopped after 13 h 20 min. Monomer conversion was found to be 69% DMA and 98% BuA (^{1}H NMR). Average molecular weight and molecular weight distribution were measured using SEC calibrated with PS standards, at final stage (M_n = 35 000 g/mol; I_p = 1.48).

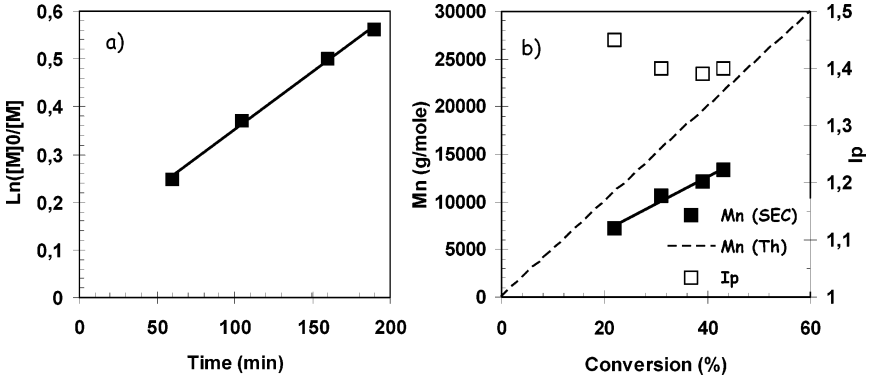

Figure 2. (a) Evolution of $Ln([M]_0/[M])$ vs time and (b) evolution of M_n vs conversion and I_p vs conversion of the polymerization of DMA carried out at 112 °C in the presence of SG1.

Results and Discussion

Homopolymerization: Synthesis of PDMA. Before the copolymerization study of DMA with BuA, we would like to ensure the possibility to control the polymerization of DMA with SG1 using the MAMA as alkoxyamine. For that, the kinetics of polymerization of DMA was achieved in order to demonstrate the ability of MAMA to control the polymerization of DMA. Indeed, the linearity observed in the plots of the logarithmic change of the monomer concentration with time (Figure 2a) indicates not only a first order with respect to the monomer, but that the growing radical concentration remained constant, which was ratified by the linear dependence of M_n with conversion (Figure 2b). Nevertheless, the intercept for the kinetic plot is not zero, which is characteristic of the fast monomer polymerization as mentioned by Gnanou and coworkers.[19] After 3 h 10 min, the reaction was stopped at 43% monomer conversion with a molecular weight $M_n = 13\,300$ g/mol and $I_p = 1.4$, determined by SEC calibrated with PEG standards.

This behavior is characteristic of a well-controlled nitroxide-mediated polymerization. Moreover, the molecular weights recorded by SEC were below those expected from theory, which can largely be attributed to the difference in hydrodynamic volume between the PDMA samples and the PEG standards used for SEC calibration. Nevertheless, the well-controlled NMP of DMA will be used to pattern gradient compositions in the macromolecular chains.

Gradient Copolymerization: Synthesis of poly(DMA-*grad*-BuA). Considering our interest in gradient copolymer by coupling antagonist intrinsic properties of two different monomers, i.e., medium/high[25] or low/high[28] glass transition temperature, we selected extremely polar and apolar monomers, i.e., a hydrophilic monomer (DMA) and a hydrophobic monomer (BuA), to synthesize a range of gradient copolymers. We carried out the synthesis of gradient copolymers by semibatch nitroxide-mediated polymerization using MAMA as an initiator and SG1 as a radical counter.

Continuously adding one monomer during a copolymerization reaction is an interesting way to form a more significant compositional gradient along the chain. By using of this method, we force the incorporation of the added monomer in the macromolecular chains. The nature as well as the structure of the gradient obtained is strictly related to the addition rate; in other terms, it is related to the change of the molar fractions of the monomeric units in the mixture feed. This synthetic methodology has been previously used to create a strong gradient composition in monomer units in an elastomer-thermoplastic copolymer.[28]

The choice of this technique for the preparation of gradient copolymers was based on the close values of the reactivity ratio between the two monomers, $r_{BuA} = 1.01 \pm 0.03$ and $r_{DMA} = 1.16 \pm 0.03$.[14] The batch copolymerization by ATRP for these monomers indicated the formation of random copolymers. For that, nitroxide-mediated polymerization combined with the forced gradient mode was used to synthesize poly(DMA-*grad*-BuA). This technique of polymerization is based on the continuous addition of DMA during the polymerization of BuA.

The composition gradient of the copolymers can be characterized through the copolymerization kinetics. Conversions of DMA and BuA as well as M_n and I_p were measured as a function of polymerization time. The DMA and BuA conversions were obtained by ^{1}H NMR versus time for three copolymerization reactions with three different additions rates.

For the gradient copolymers G_A, G_B, and G_C, the reaction was stopped at 86/76%, 62/48%, and 98/69% % conversion for BuA/DMA, respectively. The final average molecular weight and molecular weight distribution: $M_n = 33\,000$ g/mol, $I_p = 1.28$ for the gradient copolymer (G_A); $M_n = 24\,000$ g/mol, $I_p = 1.24$ for gradient copolymer (G_B); and $M_n = 35\,000$ g/mol, $I_p = 1.48$ for gradient copolymer (G_C). These values correspond to PS equivalent molecular weight (Supporting Information).

For all copolymers, the instantaneous composition is used to describe the profile of gradient copolymers. It is calculated by monitoring the conversion by ^{1}H NMR of each component during the copolymerization. This instantaneous composition was determined from the relative area of the dimethyl protons resonance of DMA ($\delta = 2.9-3.1$ ppm) and those of $O-CH_2$ ($\delta = 4.05$ ppm) protons, corresponding to BuA units. This instantaneous composition for each monomer is calculated from eq 1:

$$F_{\text{inst},1} = \frac{\Delta(\%\ \text{conv})_1[\text{M}_1]_0}{\Delta(\%\ \text{conv})_1[\text{M}_1]_0 + \Delta(\%\ \text{conv})_2[\text{M}_2]_0} \qquad (1)$$

where $(\%\ \text{conv})_1$ and $[M_1]_0$ denote the conversion and the initial concentration of monomer 1; $(\%\ \text{conv})_2$ and $[M_2]_0$ denote the conversion and the initial concentration of monomer 2.

During the synthesis of gradient copolymers, aliquots were removed throughout the reaction to verify the change in the overall fraction of DMA content by ^{1}H NMR as a function of chain length (the "delta" between subsequent samples is often larger than 15%, so the terminology used is "pseudo-instantaneous" composition). Figure 3 shows the relationship between the pseudo-instantaneous composition and the apparent normalized chain length (apparent normalized chain length is obtained from the ratio M_n/M_{nf}, where M_n and M_{nf} are the

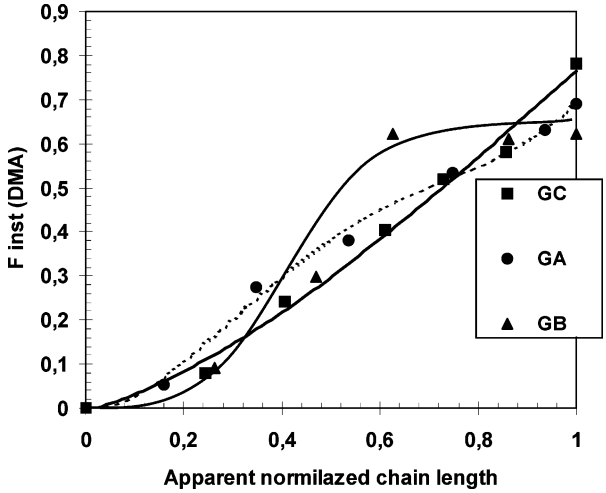

Figure 3. Evolution of DMA content in gradient copolymers as a function of the apparent normalized chain length.

molecular weights at each time and final time of polymerization, respectively). This pseudo-instantaneous fraction of the DMA increases with apparent normalized chain length for the three copolymers. It corresponds to a variation in the chemical composition in the macromolecular chains. This evolution shows that the composition of the copolymer changed clearly and gradually during copolymerization with the increase of the monomer conversions. This result confirms that the semibatch method yields easily to DMA/BuA gradient copolymers. Moreover, the variation of the pseudo-instantaneous fraction of DMA in three copolymers is not the same thanks to the three copolymers that do not have the same composition and, consequently, the same microstructure along the main chain. This demonstrates that the addition rate of monomer has a role on the incorporation of monomer in the copolymer and consequently on its microstructure. By comparison between three copolymers, we can notice an increase in the incorporation of the units of DMA with the increase of addition rate. The final composition of DMA in the three copolymers is 46, 43, and 40% for G_A, G_B, and G_C, respectively.

The increase of the DMA concentration in the mixture supports its incorporation compared to the BuA units in the macromolecular chains. These results indicated that three kinds of gradient copolymers composed of the DMA units and BuA units with different gradient shape distribution could be synthesized by controlling of the DMA addition rate.

In fact, for copolymer G_B, a typical "S" curve is obtained as described by Karaky[28] and Matyjaszewski.[29] The DMA gradient increases rapidly for apparent normalized chain lengths between 0.2 up to 0.6 and tends to a plateau characteristic of a blocky structure. This behavior seems to show that copolymer G_B presents a strong gradient, which tends to a blocky pattern with a specific monomer unit arrangement from the start to the end of the macromolecular chain. The final composition of the copolymer G_B is 43% of DMA.

On the contrary, the synthesis methodology and lower addition rate (1.4 and 0.8 mL/h) used for copolymer G_A and G_C, respectively, seems to create a continuous monomer unit gradient in the macromolecular chain. In these cases, a linear increase of DMA units in the molecular structure seems to lead to a more continuous gradient copolymer from more or less exclusively "pure" PBuA richer and richer in DMA up to final composition in DMA of 46 and 40% for G_A and G_C, respectively. This result has been also observed in the case of copolymerization of BuA in the presence of styrene.[28]

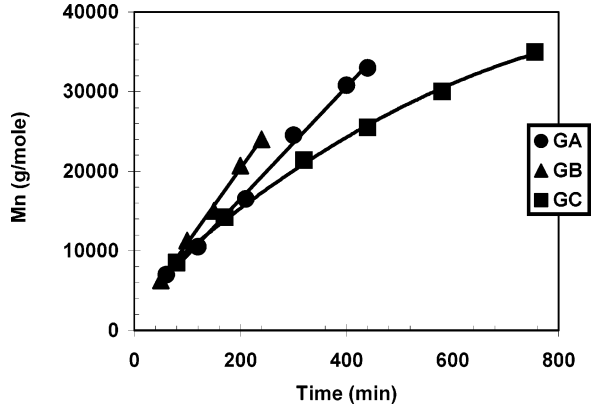

Figure 4. Evolution of M_n vs time for the gradient copolymers.

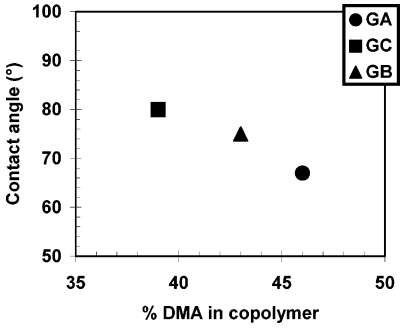

Figure 5. Static contact angle of gradient copolymers as function of percentage of DMA (%).

Moreover, in Figure 4, the molecular weight was found to increase with polymerization time for the three gradient copolymers. This increase is essential to form a gradient copolymer.

The formation of three copolymers showed the ability of SG1 combined with an alkoxyamine to control the DMA with BuA and lead to a gradient shape composition of copolymers by semibatch nitroxide-mediated polymerization patterning by different monomer addition rate.

Effect of the Gradient Shape Composition on the Surface Properties. The composition on the surface was evidenced by static contact angle measurements (θ_s). Figure 5 shows the relationship between static contact angle and the percentage of DMA in the copolymer chain. For the three copolymers, θ_s decreased as the DMA percentage increased. Moreover, the change in contact angle between the three copolymers clearly reveals that the surfaces are more hydrophilic and shows a difference between the composition on the surface and, consequently, a difference of the structure in the macromolecular chains for three gradient copolymers. This difference in the hydrophilicity may be used for surface treatments applications, in packaging or compatibilization agent, for example.

Figure 6 shows the evolution of contact angle with contact time for the PBuA and PDMA homopolymers and for the three gradient copolymers. The kinetics of surface contact angles for PBuA (hydrophobic monomer) is constant around 86°, whereas it varies between 36 and 25° for PDMA (hydrophilic monomer). This result confirms the hydrophilic character of PDMA and its ability to adsorb water or moisture. For gradient copolymers G_A, G_B, and G_C, we expected the surface would become more hydrophilic from G_C to G_A with the increase of DMA up to 46%. This behavior is clearly identified because the value of the water droplet contact angle decreases from 80° to 67°, as previously described in Figure 5.

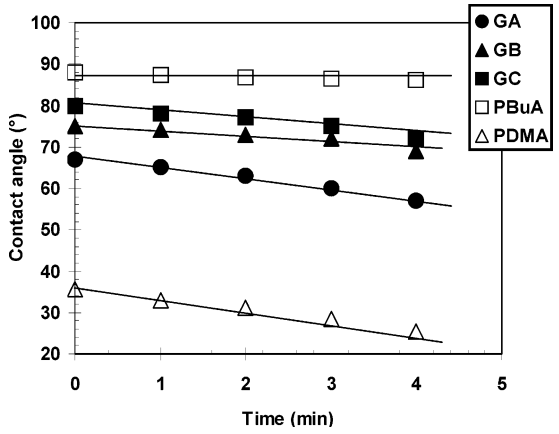

Figure 6. Static contact angle of gradient copolymers as a function of time.

Moreover, a decrease of contact angle with contact time was observed for the three gradient copolymers. This decrease depends on the composition in the macromolecular chains. Despite the close composition of DMA in the three copolymers 46, 43, and 40% for G_A, G_B, and G_C, respectively, a change of the kinetics of contact angle measurement for the three copolymers has been observed. This behavior could be partially correlated to the hydrophilic balance of each gradient copolymer; the more hydrophilic (G_A compared to G_C), the higher the kinetics of decrease of contact angle. Another important parameter for amphiphilic systems is the gradient shape profile. In such a system, if it is well-known that amphiphilic diblock copolymers form "frozen" micelles in aqueous solution, we have recently demonstrated that the gradient shape can tune the sensitivity of such micelles.[30] Indeed, if the gradient profile is slight and tends to create a homogeneous composition along the chain, the micelles are very sensitive to the water permeation inside the hydrophobic domains. On the contrary, if the gradient shape is strong and creates some blocky structure, with a abrupt "S" transition close to block copolymer profile, the water molecules cannot diffuse inside the hydrophobic phases.

Here in this present study, we can observe that the highest and the lowest rates of water penetration are observed respectively for pure PDMA ($\approx$ 2.5°/min) and gradient G_B ($\approx$ 1.4°/min). If G_B is not the more intrinsic hydrophobic gradient, it presents a strong "S" shape associated with a blocky structure, limiting thus the water diffusion in hydrophobic domains as described previously. For gradient G_A, a slight reduction of the water diffusion is calculated at around 2.3°/min, associated with its hydrophilic character but also with the smooth gradient profile permitting thus the water permeation in the small hydrophobic domains containing some hydrophilic groups ($\approx$ 0.15 of the apparent length of the chain in Figure 3). The rate of water penetration for gradient G_C is calculated at around 1.9°/min. This value is lower than the one observed for gradient G_A, even if the final composition is richer in hydrophilic domains. This behavior could be due to the presence of a longer hydrophobic segment of 0.25 of the apparent length of the macromolecular chain coupled with a hydrophobic character higher than 90% (see Figure 3).

Thermal/Rheological Properties of Gradient Copolymers. A study of the physical properties was carried out on these copolymers. DSC was used to determine the glass transition temperature T_g of these gradient copolymers, and the thermograms of G_A, G_B, and G_C are reported in Figure 7. For the G_C copolymer, two T_gs were observed, $T_{g1C} = -45.1$ °C and $T_{g2C} = 27.5$ °C. In fact, the presence of two T_gs in this gradient copolymer is related to addition rate of DMA. Indeed, by working with a low addition rate (0.8 mL/h), the concentration of BuA monomer is higher among that of DMA monomer in the initial time of the process. Consequently, we encourage first the homopolymerization of BuA at the beginning of polymerization reaction. The low T_g (−45.1 °C) corresponds to a homopolymer of PBuA,[31,32] whereas the T_g at 27.5 °C corresponds to the gradient block richer and richer in DMA up to a final composition of 40% (see Figure 3). In the case of gradient G_C, the presence of two distinct values is characteristic of a strong phase segregation in the final material with a hydrophobic phase rich in PBuA (0.25 of the apparent normalized chain length) and a second one characteristic of the gradient segment richer and richer in DMA. The same behavior has been observed for the gradient G_A with the presence of two glass transition temperatures $T_{g1A} = -27$ °C and $T_{g2A} = 8.5$ °C. Here, we can observe the presence of two values of T_g that are also characteristic of a phase segregation in the final material. These two phase transitions are associated with a difference of the composition in the main chain with a first segment rich in PBuA ($\approx$90%), corresponding up to 0.15 of the apparent normalized chain length (shorter than G_C) and a second one richer in DMA in the last part of the macromolecular chain, respectively, for T_{g1A} and T_{g2A}. Moreover, it is interesting to note that these T_{g1A} and T_{g2A} values are relatively close to each other and that the length of the first segment rich in PBuA is relatively short. For the gradient G_B, only one T_g was observed with a value $T_{gB} = -3.2$ °C. The thermogram shows an extremely broad T_g domain, which is correlated to a broad and strong variation of the concentration of the unit monomers in the macromolecular chains, as previously described in Figure 3. It means that the phase transitions are dominated by the strong "S" shape of the gradient composition, with a minor influence of the two extreme blocky segments rich in PBuA in one side and DMA in the other side.

The presence of these glass transition temperatures was confirmed by the thermomechanical measurements performed with a constant deformation pulsation (1 rad/s) within a broad temperature range. Indeed, thermomechanical characterization of the three gradient copolymers is shown in Figure 8 in the form of temperature dependencies of the real (G') and imaginary parts (G'') of the shear modulus for gradient copolymers G_A, G_B, and G_C. The dependencies indicate one extremely broad segmental relaxation for the G_B sample, indicating a broad and strong variation of the incorporation of the monomer units in the macromolecular chains. The maximum of G'' modulus corresponds to the glassy temperature noted $T_{\alpha B} = -6$ °C. This phenomena is well correlated with the behavior observed by DSC. Two distinct T_α are present in the G_C called $T_{\alpha 1C} \approx -25$ °C and $T_{\alpha 2C} \approx 30$ °C. The segmental relaxation obtained at 30 °C is extremely broad, indicating a broad variation of the incorporation of the monomers units in the macromolecular chains. The presence of two separated glassy temperatures $T_{\alpha 1C}$ and $T_{\alpha 2C}$ is in agreement with the result obtained by DSC. The difference between the values of glass transition temperatures obtained by DSC and the glassy temperature T_α obtained by rheological measure for the G_C are attributed to the difference between the temperatures ramps (2 °C·min^{-1} in rheological experiments and 20 °C·min^{-1} in DSC). For gradient G_A, we observe a broad plateau with a constant value of the imaginary G'' of 10^{+8} Pa between −20 and 10 °C and centered around −9 °C. The presence of this plateau is associated with the overlap of the two close glassy temperatures $T_{\alpha 1A}$ and $T_{\alpha 2A}$ observed by DSC. In this experiment, the two transitions are

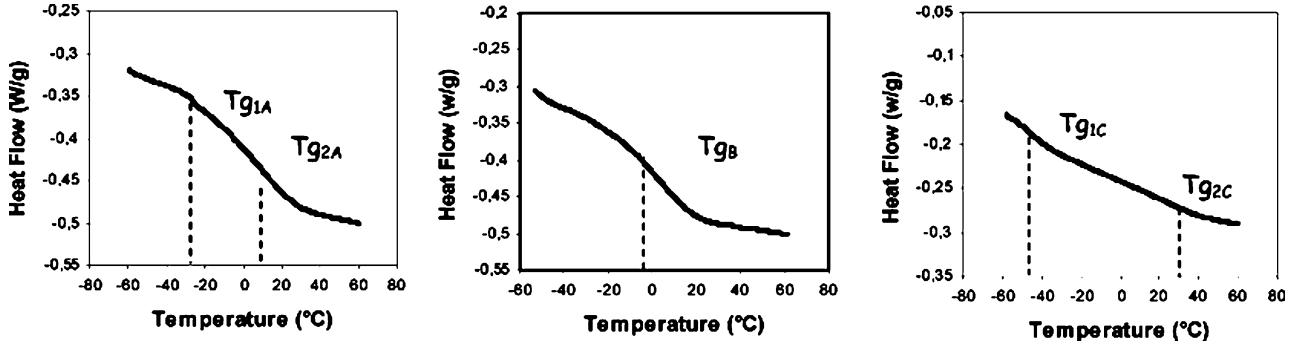

Figure 7. DSC thermograms for gradient copolymers G_A, G_B, and G_C, from left to right (see Supporting Information).

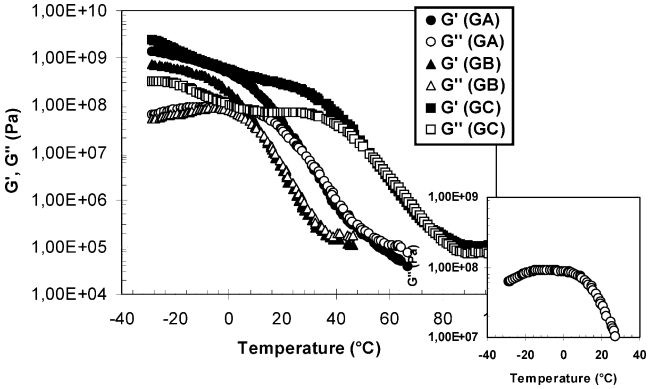

Figure 8. Temperature dependencies of the real G' and imaginary G'' parts of the shear modulus for DMA/BuA gradient copolymers (inset: zoom of the imaginary G'' of the gradient G_A).

not separated but appear as a broad transition (inset, Figure 8).

Moreover, we can observe a maintenance of the rheological modules for the copolymer G_c at high temperature even after the glass transition temperature of the sequence richer in PBuA. Such behavior is characteristic of the presence of a separation phase characterized by the coexistence of "soft" elastomer pure PBuA phase and "hard" amphiphilic thermoplastic PBuA-*grad*-PDMA phase. This result could be very interesting because such gradient copolymers could be plasticized under specific and controlled conditions to tune their adhesion properties. In this case, because of the value of $T_{\alpha C2}$ close to the human body temperature ($\approx$ 30 °C), these properties, especially adhesion, could be controlled by the contact with skin moisture.

Effect of the Gradient Shape Composition on the Surface Organization. In the previous paragraphs, we have shown the effect of gradient shape composition on the surface but also bulk properties. One other interesting effect could be on the surface organization of these new polymeric materials. As we have recently described for styrene/butyl acrylate system, gradient copolymers can be organized and self-assembled in bulk soft matter in order to create a new type of nanostructured polymeric material.[28] To compare the influence of the gradient shape composition on the surface organization, we have also used a diblock copolymer P(DMA-*b*-BuA) synthesized by NMP from a PBuA of molecular weight 22 000 g·mol^{-1} with a polydispersity index of 1.33. This block copolymer is characterized by a molecular weight of 33 000 g·mol^{-1} with a polydispersity index of 1.28 and a composition of 58/42, respectively, in PDMA/PBuA (^{1}H NMR). By DSC, this block copolymer presents a phase segregation with two glass transitions at −44 °C and 115 °C, respectively, for the pure sequences of PBuA and PDMA.

The study of surface morphology of the gradient copolymers was carried out by atomic force microscopy (AFM) on thin films obtained by spin-coating (Figure 9). In Figure 9 (left), we can observe the top surface organization of the diblock copolymer with the formation of PBuA nodules in a PDMA continuous matrix. Because of the monomer composition, the DMA is the majority monomer that forms the continuous phase of these materials. The radius nodule size is around 250 nm, and a few coagulation of elastomer nodules can be observed with the formation of "peanuts" nodules on the extreme surface. When the proportion of DMA decreases in the macromolecular chain composition, the nodular organization shifts to the lamellar phase, as observed in Figure 9 (middle) with the gradient copolymer G_A (PDMA/PBuA = 46/54). In this case, the radius of the lamella increases strongly to 750 nm. Moreover, from this type of gradient, we can also observe a gradient structure from the center (richer in BuA: black zone) through the middle (strong gradient: gray zone) and finally to the outer shell (richer in DMA: white zone) of each lamella. This behavior could be associated to the presence of two distinct phase transitions observed for gradient G_A by DSC and rheology. If the proportion of DMA always decreases along the main chain as for gradient G_C, we observe a phase inversion with nodules rich in PDMA in a matrix richer in PBuA (Figure 9, right). In this case, the

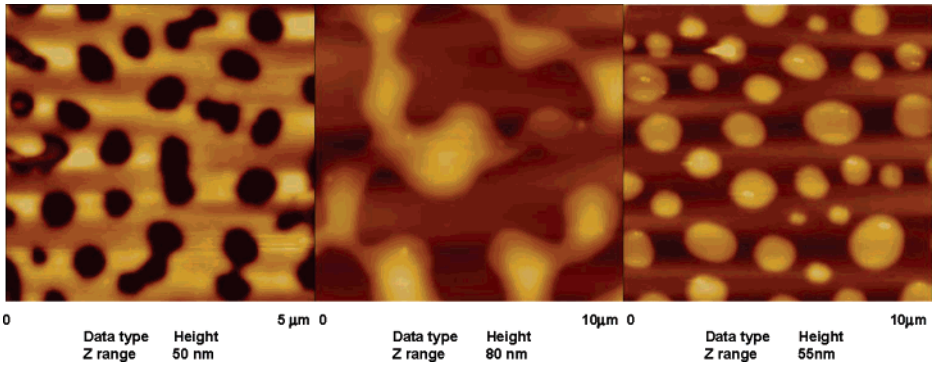

Figure 9. AFM images of block copolymers gradients G_A and G_C, respectively, from left to right.

nodules size increases to 400 nm due the gradient sequence of the macromolecular chain, increasing the miscibility between the two chains ends rich in PBuA and PDMA. No gradient can be observed between the nodule centers and the matrix because the strong composition variation in the macromolecular chains close to a block copolymer segregation (see Figure 3 and Figure 9, left). Moreover, these nodules are characteristic of the presence of a strong phase separation, as previously observed with thermal/rheological properties, with two well-distinct glass transitions lower and upper than those at room temperature. For the gradient G_B, because of the presence of only one glass temperature lower than room temperature and to the sticky behavior of such copolymer, no images have been performed.

This study presents here for the first time, a submicron phase separation in gradient copolymers observed by AFM technique. These gradient copolymers behave as a block copolymer when the total composition varies around 50%. Nevertheless, it seems that it could be possible to visualize the gradient composition when the composition variation gradually changes along the main chain. With an "S" composition curve, the transition between the chain ends is too fast and this gradient copolymer presents the same organization as pure block copolymer. This surface characterization by AFM represents a preliminary study that opens a new class of amphiphilic copolymers. Indeed, the moisture influence study on these types of copolymers compared to block copolymers are underway to check the variation of the water-sensitive structures.

Conclusion

In this paper, we reported the synthesis of well-defined PDMA by nitroxide-mediated radical polymerization using for the first time an alkoxyamine. We also demonstrated the synthesis of gradient copolymers of poly(DMA-*grad*-BuA) with different gradient shapes depending on the addition rate of DMA. The SG1 used as control agent combined with an alkoxyamine (MAMA) as initiator provided a well-controlled copolymerization. The influence of addition rate on the shapes and the structures of gradient copolymers were demonstrated. The semibatch polymerization with a low addition rate (0.8 mL/h) leads to the synthesis of gradient copolymer from the macroinitiator of PBuA. These gradient copolymers demonstrate interesting rheological properties. Moreover, thanks to the combination of DMA (hydrophilic monomer)/BuA (monomer having a low T_g) and to the formation of phase segregation as observed by AFM, these systems will be used in the treatment of surfaces, for example, adsorption of moisture, thanks to the hydrophilic properties of DMA.

Acknowledgment. We gratefully acknowledge financial support from FNADT, FEDER, CG Pyrénées Atlantique, and Association "2PSM", and their directors J. Francois and P. Maury for their support and motivation. C. Derail is also thanked for discussion on rheological measurements.

Supporting Information Available: Kinetics of gradient copolymers in semibatch NMP at different addition rates and zoom on gradient copolymers DSC thermograms This material is available free of charge via the Internet at http://pubs.acs.org.

References and Notes

(1) Shalaby, S. W.; McCormick, C. L.; Butler, G. B. *Water-Soluble Polymers: Synthesis, Solution Properties, and Application.* ACS Symposium Series 467; American Chemical Society: Washington, DC, 1991.
(2) Mark, H. F.; Gaylord, N. G.; Bikales, N. *Encyclopedia of Polymer Science Technology*; Wiley and Sons: New York, 1964; Vol. 1.
(3) (a) Kathmann, E. E. L.; White, L. A.; McCormick, C. L. *Macromolecules* **1997**, *30*, 5297.
(4) Konak, C.; Oupicky, D.; Chytry, V.; Ulbrich, K.; Helmestedt, M. *Macromolecules* **2000**, *33*, 5318.
(5) Wang, J. S.; Matyjaszewski, K. *J. Am. Chem. Soc.* **1995**, *117*, 5614.
(6) Coessens, V.; Pintauer, T.; Matyjaszewski, K. *Prog. Polym. Sci.* **2001**, *26*, 337.
(7) Matyjaszewski, K.; Xia, J. *Chem. Rev.* **2001**, *101*, 2921.
(8) Kamigaito, M.; Ando, T.; Sawamoto, M. *Chem. Rev.* **2001**, *101*, 3689.
(9) Rizzardo, E.; Chiefari, J.; Mayadunne, R. T. A.; Moad, G.; Thang, S. H. *Macromol. Symp.* **2001**, 174.
(10) Baum, M.; Brittain, W. J. *Macromolecules* **2002**, *35*, 610.
(11) Donovan, M. S.; Lowe, A. B.; Sumerlin, B. S.; MCCormick, C. L. *Macromolecules* **2002**, *35*, 4123.
(12) Donovan, M. S.; Sanford, T. A.; Lowe, A. B.; Sumerlin, B. S.; Mitsukami, Y.; McCormick, C. L. *Macromolecules* **2002**, *35*, 4570.
(13) Coessens, V.; Pintauer, T.; Matyjaszewski, K. *Prog. Polym. Sci.* **2001**, *26*, 337.
(14) Neugebauer, D.; Matyjaszewski, K. *Macromolecules* **2003**, *36*, 2598.
(15) Senoo, M.; Kotani, Y.; Sawamoto, M. *Macromolecules* **1999**, *32*, 8005.
(16) Chong, Y. K. (Bill); Le, T. P. T.; Moad, G.; Rizzardo, E.; Thang, S. H. *Macromolecules* **1999**, *32*, 2071.
(17) Li, D.; Brittain, W. J. *Macromolecules* **1998**, *31*, 3852.
(18) Diaz, T.; Fischer, A.; Jonquières, A.; Brembilla, A.; Lochon, P. *Macromolecules* **2003**, *36*, 2235.
(19) Schierholz, K.; Givehchi, M.; Fabre, P.; Nallet, F.; Papon, F.; Guerret, O.; Gnanou, Y. *Macromolecules* **2003**, *36*, 5995.
(20) Arehart, S. V.; Greszta, D.; Matyjaszewski, K. *Polym. Prepr. (Am. Chem. Soc., Div. Polym. Chem.)* **1997**, *38*, 705.
(21) Haddleton, D. M.; Crossman, M. C.; Hunt, K. H.; Topping, C.; Waterson, C.; Suddaby, K. G. *Macromolecules* **1997**, *30*, 3992.
(22) Ziegler, M. J.; Matyjaszewski, K. *Macromolecules* **2001**, *34*, 415.
(23) Lee, S. B.; Russell, A. J.; Matyjaszewski, K. *Biomacromolecules* **2003**, *4*, 1386.
(24) Min, K.; Li, M.; Matyjaszewski, K. *J. Polym. Sci., Part A: Polym. Chem.* **2005**, *43*, 3616.
(25) Karaky, K.; Pere, E.; Pouchan, C.; Desbrières, J.; Khoukh, A.; Francois. J, Billon, L. *New J. Chem.* **2006**, *30*, 698.
(26) Hu, Z.; Zhang, Z. *Macromolecules* **2005**, *36*, 1384.
(27) Kotani, Y.; Kamigaito, M.; Sawamoto, M. *Macromolecules* **1998**, *31*, 5582.
(28) Karaky, K.; Pere, E.; Pouchan, C.; Desbrières, J.; Derail, C.; Billon, L. *Soft Matter* **2006**, *2*, 770.
(29) Matyjaszewski, K.; Ziegler, M. J.; Arehart, S. V.; Greszta, D.; Pakula, T. *J. Phys. Org. Chem.* **2000**, *13*, 775.
(30) Laruelle, G.; Borisov, O.; Lapp, A.; Francois, J.; Billon, L. *Polym. Prepr. (Am. Chem. Soc., Div. Polym. Chem.)* **2006**, *47*, 775.
(31) Inoubli, R.; Dagreou, S.; Lapp, A.; Billon, L.; Peyrelasse, J. *Langmuir* **2006**, *22*, 6683.
(32) Ghannam, L.; Garay, H.; Francois, J.; Shanahan, M. E. R.; Billon, L. *Chem. Mater.* **2005**, *17*, 3837.

MA062456S